Catalytically Active Species in Copper/DiPPAM-Catalyzed 1,6-Asymmetric Conjugate Addition of Dialkylzinc to Dienones A Computational Overview

Stéphanie Halbert, Jimmy Lauberteaux, Charlie Blons, Renata Marcia de Figueiredo, Christophe Crévisy, Olivier Baslé, Jean-Marc Campagne, Marc Mauduit, Hélène Gérard

▶ **To cite this version:**

Stéphanie Halbert, Jimmy Lauberteaux, Charlie Blons, Renata Marcia de Figueiredo, Christophe Crévisy, et al.. Catalytically Active Species in Copper/DiPPAM-Catalyzed 1,6-Asymmetric Conjugate Addition of Dialkylzinc to Dienones A Computational Overview. ChemCatChem, 2019, 11 (16), pp.4108-4115. 10.1002/cctc.201900233 . hal-02181830

HAL Id: hal-02181830
https://univ-rennes.hal.science/hal-02181830v1

Submitted on 9 Sep 2019

HAL is a multi-disciplinary open access archive for the deposit and dissemination of scientific research documents, whether they are published or not. The documents may come from teaching and research institutions in France or abroad, or from public or private research centers.

L'archive ouverte pluridisciplinaire **HAL**, est destinée au dépôt et à la diffusion de documents scientifiques de niveau recherche, publiés ou non, émanant des établissements d'enseignement et de recherche français ou étrangers, des laboratoires publics ou privés.

Catalytically active species in Copper/DiPPAM-Catalyzed 1,6-Asymmetric Conjugate Addition of Dialkylzinc to Dienones: a computational overview.

Stéphanie Halbert,[a] Jimmy Lauberteaux,[b] Charlie Blons,[c] Renata Marcia de Figueiredo,[b] Christophe Crévisy,[c] Olivier Baslé,[c] Jean-Marc Campagne,[b] Marc Mauduit*[c] and Hélène Gérard.*[a]

Abstract: Four different catalytically active species are computationally examined in order to investigate the mechanism of Cu/DiPPAM-catalyzed 1,6-conjugate addition of dialkylzinc to acyclic dienones. A DiPPAM–bridged Cu(alkyl)-Zn(acetate) bimetallic complex exhibits the best catalytic activity, which can be associated with the best balance between the stability of the dienone adduct and its activation by copper. The selectivities (regio- and enantioselectivity) associated with the retained mechanism are investigated by DFT calculations and successfully compared to experimental data, including the critical influence of the substituents within the dienone on the regioselectivity and the obtained enantioselectivity for the formation of one 1,6-adduct.

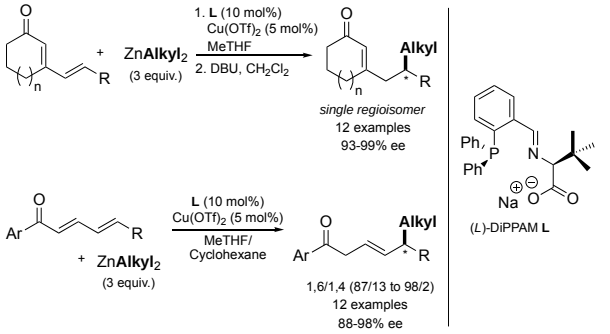

Scheme 1. $Cu(OTf)_2$/DiPPAM **L** efficiently catalyzed 1,6-ACA of dialkylzinc reagents to cyclic and acyclic $\alpha,\beta,\gamma,\delta$-dienones.

Introduction

Copper-catalyzed Asymmetric Conjugate Addition (ACA) to electro-deficient substrates is an efficient method to form C-C bonds.[1,2] The 1,6-addition to $\alpha,\beta,\gamma,\delta$-dienone is especially challenging, as a complete regiocontrol is difficult to reach because of the presence of numerous active sites. However, 1,6-ACA has been described with a range of electrophiles, nucleophiles, metal-based catalysts, and chiral ligands families.[3–9] Mauduit *et al.* have developed an efficient chiral tridentate P,N,O ligand, named DiPPAM (DiPhenylPhosphinoAzoMethinylate salt **L**),[10] which has proved its efficiency for copper-catalyzed 1,6-ACA of dialkylzinc reagents to cyclic [5,7] and more recently to acyclic[11–13] dienones (Scheme 1). While good to excellent regioselectivity and enantioselectivity could be achieved with this catalytic system, attempts to characterize intermediates were unsuccessful and the active catalytic species has remained unidentified.

On the other hand, mechanistic investigations on conjugate addition were previously undertaken in the case lithium organocuprate as nucleophiles, resorting on kinetic[14] NMR spectroscopy[15–18] studies. The rate-determining step is the C-C bond formation as described by investigations on kinetic isotope effects and activation parameters. In addition, the formation of a π-complex between copper and C=C bond was predicted by NMR studies.[17,19,20] These data are completed by computational studies.[21–26] The mechanism comprises different steps: the formation of the lithium organocuprate, the coordination of the carbonyl compound as a π-complex, an oxidative addition to form a Cu(III) intermediate (Figure 1, a), followed by a reductive elimination corresponding to the C-C bond formation.

For Cu-catalyzed ACA, the nature of the catalytically active species becomes a major issue. Whereas a Cu(II) salt is generally used as the precatalyst, a Cu(I) complex is considered to be the active species,[1] in line with NMR and EPR evidences supporting the reduction of Cu(II) to Cu(I).[27] In this context, a halide-bridged bimetallic monocopper is proposed for bidentate phosphine ligand (Josiphos) when resorting to a Grignard reagent (EtMgBr) as an alkyl source (Figure 1, b).[28] A similar intermediate was more recently described within the framework of the first direct experimental detection of transmetalation intermediates in copper-catalyzed addition reaction using the monodentate phosphoramidite ligand and diethylzinc as nucleophile.[29] Nevertheless, another bimetallic intermediate was detected in the latter study, this time exhibiting two Cu centers and three phosphine ligands. Two Cu centers are also present in the [Zn(μ-X)Cu(μ-X)CuR] trimetallic structure proposed as a catalytically active species (Figure 1, c) from a computational point of view by Calhorda *et al.* In this case, inter-metallic bridge X can be a variety of suitable ligand, like an acetate (or thiophene carboxylate, triflate, ...).[30]

[a] Dr. S. Halbert, Pr. Dr. H. Gérard
Sorbonne Université, CNRS, Laboratoire de Chimie Théorique, F-75252 Paris, France.
E-mail: helene.gerard@sorbonne-universite.fr
[b] J. Lauberteaux, Dr. R. Marcia de Figueiredo, Pr. Dr. J.-M. Campagne
Institut Charles Gerhardt Montpellier, UMR 5253 CNRS-UM-ENSCM, Ecole Nationale Supérieure de Chimie de Montpellier, 8 Rue de l'Ecole Normale, 34296 Montpellier Cedex 5, France
[c] C. Blons, Dr. C. Crévisy, Dr. O. Baslé, Dr. M. Mauduit
Univ Rennes, Ecole Nationale Supérieure de Chimie de Rennes, CNRS, ISCR - UMR 6226, F-35000 Rennes, France
E-mail: marc.mauduit@ensc-rennes.fr

Supporting information for this article is given via a link at the end of

Accepted Manuscript

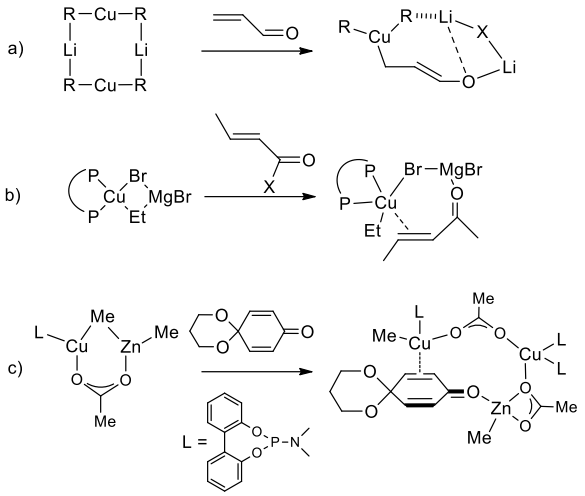

Figure 1. Proposed intermediates in conjugate addition reaction with lithium organocuprate cluster (a), with halide-bridged bimetallic monocopper (b) and with trimetallic specie (c) from computational studies.

Having these features in mind, our group has recently proposed a mechanism for Cu-catalyzed ACA of dialkylzinc to dienones using anionic and chiral ligands as a bridge between the Cu and Zn centers.[31,32] This model was found to be applicable to a variety of ligands (Figure 2, a), as both DiPPAM **L** or hydroxylalkyl N-Heterocyclic Carbene ligands (**NHC**), and to different electrophiles (cyclic and acyclic dienones with various substituents). The relevance of this catalytic active species was supported by the good agreement with selectivity between experimental observations and calculations. Indeed, it was used to rationalize the effect of the nature of the substituent at C=O position in substrate on the regioselectivity towards 1,4- or 1,6-conjugate addition,[31] evidencing the possibility for an electron-rich substituent (methyl-imidazole for instance) to establish an interaction with the electro-deficient copper. The same model also allowed to reproduce and analyze the enantioselectivity of the ACA, which was proposed to originate from a stabilizing π-stacking network in the π-complex.[32] Nevertheless, no experimental or computational evidences were available to support the nature of the postulated intermediates.

In this paper, we aim at determining the origin of the catalytic activity through comparison of various reaction mechanisms. In a first part, the origin of the regio- and stereo-control is determined for ACA of $ZnEt_2$ on acyclic α,β,γ,δ-dienone, a more challenging than the previously examined ones due to its increased versatility (Figure 2). In a second part, alternative catalytically active species, resulting in alternative catalytic effects, are examined. It allows us altogether to confirm our mechanistic hypothesis and to evaluate the potential (or risk) of emergence of competitive pathways under different reaction conditions.

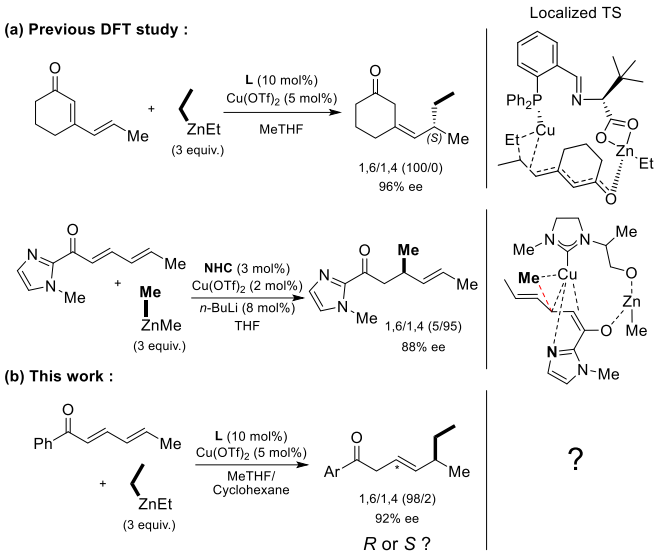

Figure 2. DFT study on 1,6 *vs* 1,4 selectivity of Cu-ACA of dialkylzincs to α,β,γ,δ-unsaturated Michael acceptors: (a) previously reported and (b) this work.

Results and Discussion

Regio- and enantio-selectivity in acyclic ketones.

The copper-catalyzed asymmetric addition of $ZnEt_2$ to (3*E*,5*E*)-trideca-3,5-dien-2-one (**1**) had previously been experimentally investigated using L-DiPPAM **L** (Table 1).[11] Two dienones were considered which differ by the groups at terminal position (R^1) and at C=O function (R^2). When the reaction was performed at room temperature with **1a**, very good regioselectivity (98:2) with good yield (70%) was obtained in favor of the 1,6-product with a large enantiomeric excess (92%). When the positions of the methyl and phenyl groups were exchanged (**1b**), very different results were obtained as both yield (30%), regioselectivity (30:70) and enantioselectivity (53% ee) were found to be moderate. We thus undertook a systematic study of the reaction path in **1a** to better determine the origin of the excellent selectivities.

Table 1. Cu/DiPPAM-catalyzed enantioselective 1,6-addition of $ZnEt_2$ to linear dienones.[11]

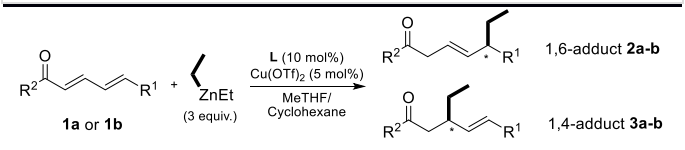

Dienone	R^1/R^2	**2**/**3** ratio	Yield[c] [%]	ee [%]
1a	Me/Ph	98:2	70	92
1b	Ph/Me	30:70	37	53[a]

[a]For the 1.4-adduct

Accepted Manuscript

Similarly to our previous studies as well as in the study reported by Nakamura *et al.*,[33] the C-C bond formation step takes place in a bimetallic species (Figure 3 and Table S1, for detailed geometrical parameters in SI), in which DiPPAM ligand is the only bridge between Cu and Zn centers. As Zn(II) is coordinated to the carboxylate arm and an alkyl chain, whereas Cu(I) is bonded to the phosphine site and another alkyl chain, this heterobimetallic species is formally composed of two neutral metal centers. Bonding of the electrophile (1a) at the Zn(II) center through one of the carbonyl lone pair is referred to I_0. An additional binding is observed as the C=C bond of 1a comes into interaction through a π-bond with the Cu(I) center, resulting in intermediate I_4 when 1,4-conjugate addition is examined, and I_6 in the case of 1,6-conjugate addition. I_6 and I_0 intermediates are in equilibrium as they are isoergonic, with an exchange between the two structures exhibiting a Gibbs free energy equal to 13 kcal.mol^{-1} which proved to be lower than the C-C bond formation step. In contrast, I_4 is found to be significantly destabilized (ΔrG = + 7.2 kcal.mol^{-1}) and its formation is disfavored ($TS_{\pi 4}$ higher than C-C bond formation in $TS_{C\text{-}C6}$).

The C-C bond formation profile (in red for 1,4- and in blue for 1,6-conjugate addition in Figure 3) clearly suggests that the most favorable pathway is the 1,6-conjugate addition from both thermodynamic (as the enolate product **P_6** is more stable than **P_4** by 7.2 kcal.mol^{-1}) and kinetic (as **$TS_{C\text{-}C6}$** is lower than **$TS_{C\text{-}C4}$** by more than 10 kcal.mol^{-1}) points of view. It is in line with previous theoretical studies for addition of Me group at the terminal C=C bond of penta-2,4-dienal in a cuprate aggregate model.[34] This can be associated to the loss of conjugation during the 1,4-addition, which is already well advanced in **$TS_{C\text{-}C4}$**, as highlighted by the evolution of the Cα=Cβ bond length along the 1,4-addition pathway (1.36 Å in **I_0**, lengthened to 1.42 Å through formation of the π-adduct in **I_4**, quasi-single with 1.47 Å in **$TS_{C\text{-}C4}$** compared to 1.53 Å for the Cα-Cβ single bond in the product **P_4**). These conjugation effects fully justify the strong difference observed between **1a** to **1b**. In **1b**, in the case of 1,6-addition, the C-C bond formation fully breaks the conjugation of the phenyl group with the π system whereas, in the 1,4-addition, conjugation of the terminal C=C bond with Ph is kept. Conjugation is thus proposed to be the factor tuning regioselectivity between **1a** and **1b**, in parallel to the already observed ligand effects (reported for BINAP)[11] or to the additional substrate-catalyst interaction (reported for Acyl-N-methylimidazole).[31] This is confirmed by computations on a simple model including only electronic effects in **1a** and **1b** (see Tables S2-S4 in SI).

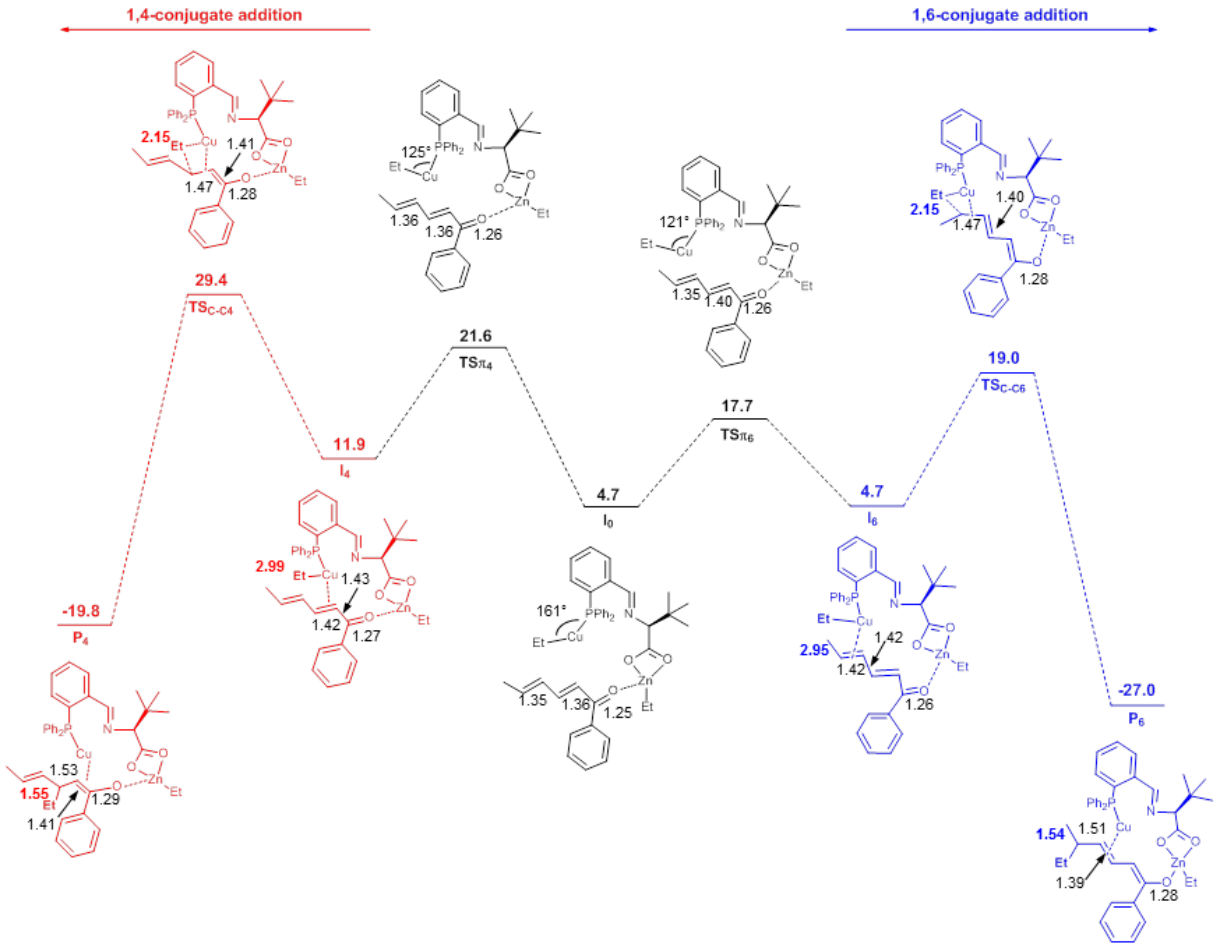

Figure 3. DFT calculations on the regioselectivity of the copper-catalyzed addition of diethylzinc to α,β,γ,δ-unsaturated dienone 1a (R^1=Me ; R^2=Ph): Gibbs free energy (in kcal.mol^{-1}) profile of the C-C bond formation steps relative to separated Cu(L-DiPPAM), $ZnEt_2$ and 1a.

Accepted Manuscript

We next investigate the origin of the enantioselectivity of the 1,6-addition to dienone **1a** using the previously reported results showing that it is possible to predict the experimentally formed enantiomer from the stability of adduct $\mathbf{I_6}$.[35]

Such an approach proved efficient in the case of cyclic dienone in agreement with the VCD and X-ray data,[32] provided an adapted computational level (dispersion correction was added to DFT calculations, see Computational Details) and an adapted docking procedure are used. Indeed, it appeared necessary to envision not only the two potential docking sides of the Cγ=Cδ double bond, but also all possible conformations relative to the C(O)-Cα and Cβ-Cγ bonds, as the most stable structure of the free ketone is not necessarily the one preferred in the bimetallic π-complex. In the case of acyclic ketones, a similar study was thus undertaken, which required investigation of a larger number of conformers as both C(O)-Cα and Cβ-Cγ single bonds can afford both s-cis and s-trans conformations (Figure 4).

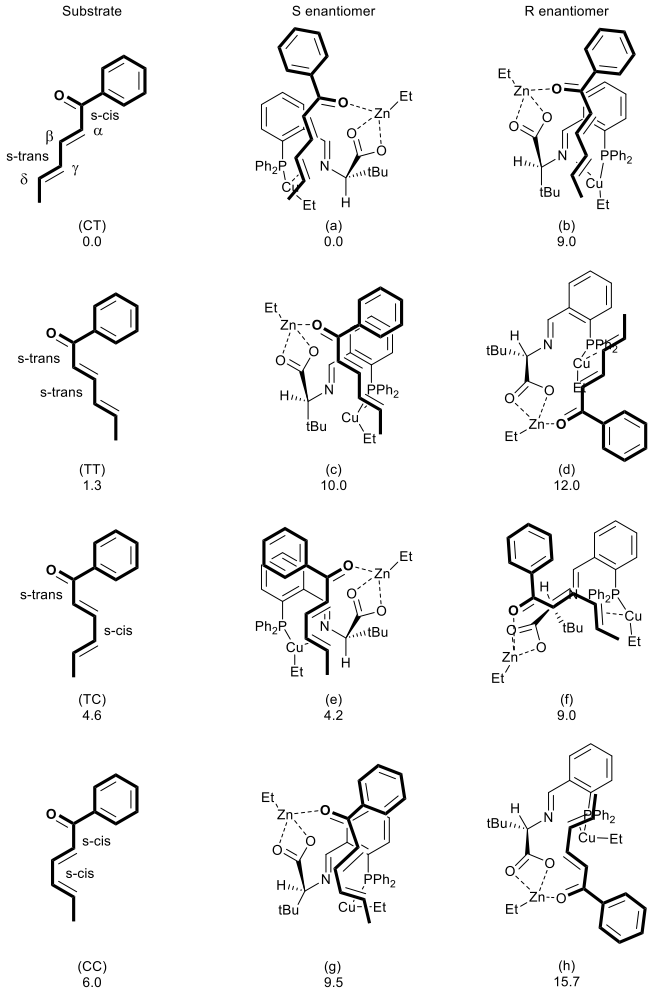

Figure 4. Eight possible structures computed for $\mathbf{I_6}$ with **L** = L-(*S*)-DiPPAM and acyclic dienone **1a** in the various conformations of the C-C single bonds. Structures on the left yield the *S* enantiomer and those on the right lead to the *R*. Energies (in kcal mol^{-1}) are given with respect to structure (a).

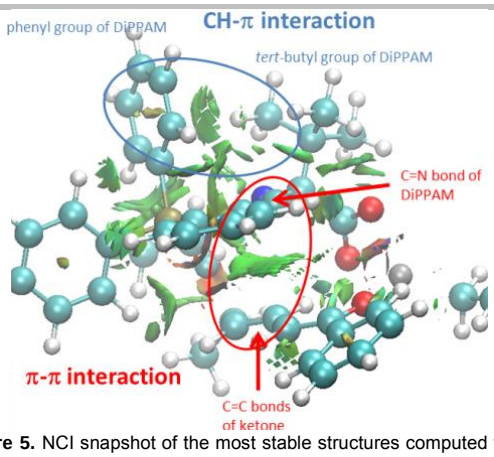

Figure 5. NCI snapshot of the most stable structures computed for I_6 with L = L-(S)-DiPPAM and acyclic dienone **1a** (structure (a) in Figure 4)

Eight structures of the π-complex $\mathbf{I_6}$ were computed, corresponding to the two docking sides for the four possible conformations of the substrate, introduced in Figure 4 and noted CT, TT, TC and CC. These structures are expected to be in fast equilibrium, considering the high C-C bond formation barriers compared to the coordination/decoordination of the ketone to the bimetallic complex reported above. The CT conformer is the most stable for the free dienone (by 1.3 kcal.mol^{-1} compared to the TT analogue). This preference is conserved in $\mathbf{I_6}$ intermediates. The most stable arrangement calculated is affiliated with the formation of the *S*-enantiomer (structure (a) in Figure 4) and this strong (> 4 kcal.mol^{-1}) preference is conserved when adding entropic contributions (See SI, Figure S1). An NCI analysis, given in Figure 5, allows determination of the origin of this preference thanks to the observation of two characteristic non-bonding isosurfaces. This conformer seems to be stabilized by CH-π interaction between the C-H bond of *tert*-butyl group and a phenyl group of diphenylphosphino moiety. A second π-π interaction is observed between C=C bond of substrate and imine group of DiPPAM ligand. This network of CH-π interactions (in SI, Figure S2) is similar to that obtained in the intermediate with cyclic dienone.[32]

As conclusion, the enantioselectivity of the addition is controlled by two main non-covalent interactions, one ensuring the folding of the DiPPAM ligand (CH-π interaction) and one associated with the docking of the ketone and related to the interaction of its unsaturated π system with the C=N bond of DiPPAM.

An experimental derivatization was initiated to confirm the enantioselectivity obtained from DFT calculations. In order to access to the absolute configuration of **2a** obtained from Cu/L-DiPPAM catalyzed 1,6-ACA to **1a**, the former was converted to the known ester **4**[36] following a slightly modified described procedure (Scheme 2 and Experimental Section).[37]

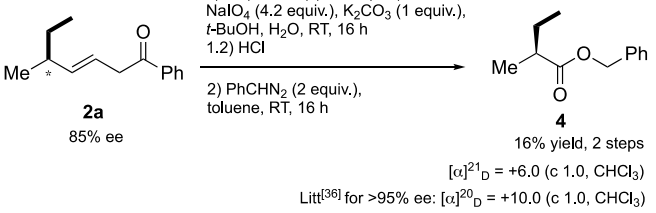

Scheme 2. Experimental process to determine the absolute configuration of **2a**.

Accepted Manuscript

The literature reported an *S* absolute configuration with a positive rotation ($[\alpha]_D^{20}$ = +10.0 (c 1.0, $CHCl_3$)).[36] In our case, compound **4** obtained from **2a** have the same sign, confirming *S* is the major enantiomer for **2a.** The evaluated value for $[\alpha]_D^{21}$ = +6.0 (c 1.0, $CHCl_3$) is consistent with 85% ee obtained for **2a**. Thus, a (*S*) configuration can be assigned to compound **2a**, in accordance to the calculated data.

Alternative mechanisms.

The mechanism proposed above, based on the similarity with previous studies,[21–26] nicely confronts to experimental selectivity data (regio- and enantio-selectivity). It nevertheless relies on a catalytically active species (bimetallic Cu-Zn complex of DiPPAM) which could not be characterized through experimental analysis. We thus decided to undertake theoretical mechanistic investigations of the 1,6-addition pathway to understand the electronic factors governing the formation and activation with this catalytic intermediate. This interpretative part of the theoretical study was carried out using models compounds including all electronic effects but minimizing steric ones: $ZnMe_2$ is reacted in the presence of a copper (I) complex and a model of DiPPAM ligand (**M**), for which the *tert*-butyl group as well as the phenyl group at the phosphine are replaced by hydrogen atoms. This small model provides similar result to the full one in the case of the addition to 1a (Figure S3 and Table S5).

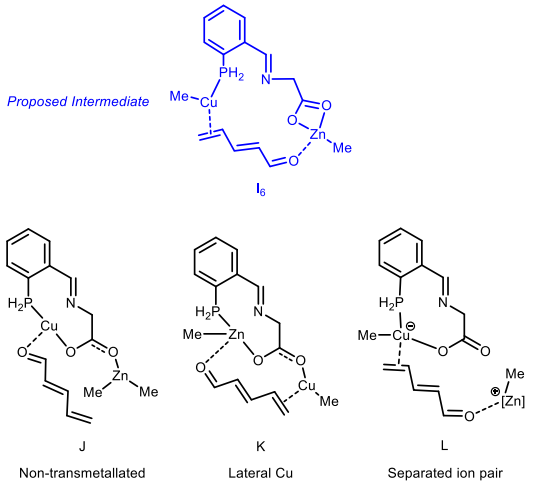

Figure 6. Proposed alternative intermediates. [Zn] refers to Zn(II) coordinated to explicit solvent molecules (taken as OMe_2).

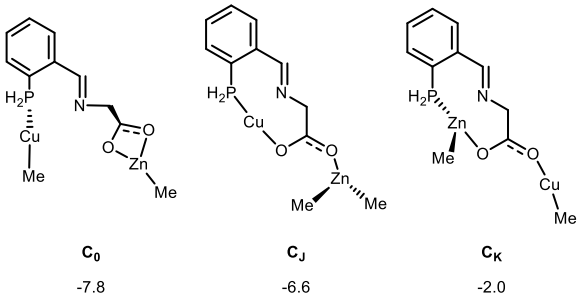

Figure 8. Optimized intermediates without docking of dienone (energies are given relative to the separated reactants **Cu(M)** + $ZnMe_2$)

Three alternative mechanisms are envisioned for the 1,6-conjugate addition. The first one (going through intermediate **J**, Figure 6) is deduced from direct interaction of the $ZnMe_2$ with a preformed **Cu(M)** complex without methyl transfer from Zn to Cu: Cu is thus bonded to the phosphine chain of the DiPPAM whereas $ZnMe_2$ interacts with the carboxylate arm. The second one (**K** in Figure 6) is similar to $\mathbf{I_0}$ except for the exchange of the Cu and Zn binding sites. The last one is obtained from $\mathbf{I_6}$ through decoordination of the $ZnMe^+$ center from the carboxylate arm of the DiPPAM to form a separated ion pair (**L** in Figure 6). Detailed studies of the energetics and structural features associated to these three mechanisms are next reported. (Figure 7, complete data in SI, Tables S5-S6). In order to better characterize the docking of the dienone in the intermediates given in Figure 5, the associated Cu-Zn bimetallic complexes have also been optimized (Figure 8).

Mechanism through J. The docking of the carbonyl compound to **Cu(M)** forms intermediate noted $\mathbf{I_J}$ in Figure 7, b. As expected, no interaction of Zn center with C=C bond could be obtained.[38] In this case, Cu plays the role of Lewis acid while Zn acts as a Me donor. The sole coordination energy of the C=O bond to copper in $\mathbf{I_J}$ can be evaluated relative to $\mathbf{C_J}$ to -6.6 kcal.mol^{-1}. In contrast, substrate binding to $\mathbf{I_6}$ combines a coordination of the C=O to Zn and of the C=C to copper, leading to an overall interaction energy computed with respect to $\mathbf{C_0}$ of -11.1 kcal.mol^{-1}. It is found to be the quasi-additive contribution of the sole coordination of the C=O to Zn in $\mathbf{I_0}$ (ΔE = -6.6 kcal mol^{-1} with respect to $\mathbf{C_0}$) and of the binding of the double bond to Cu (-3.9 kcal mol^{-1} for binding of ethylene to (Me)**Cu(M)**).[39] Intermediate $\mathbf{I_6}$ allows thus both a good coordination of the C=O to the metal center and a significant coordination of the π system to Cu. Let us nevertheless notice that the strong binding of the carbonyl compound in $\mathbf{I_6}$ is associated with a large entropic loss compared to $\mathbf{I_J}$, for which more degrees of freedom of the carbonyl chain are kept. As a consequence, similar Gibbs energies with respect to separated reactants were found for $\mathbf{I_6}$ and $\mathbf{I_J}$ (7.2 kcal.mol^{-1}). Discrimination between these two mechanisms thus originated from kinetic factors. The activation barrier in the non-transmetalated mechanism is equal to 27.2 kcal.mol^{-1} relative to $\mathbf{I_J}$, so that $\mathbf{TS_J}$ is significantly higher than $\mathbf{TS_{C\text{-}C6}}$ (in Figure 7, a, associated with 17.5 kcal.mol^{-1} barrier). $\mathbf{TS_J}$ is found to be a little more reactant-like, as evidenced from the shorter $C\gamma{=}C\delta$ bond (1.403 Å in $\mathbf{TS_J}$ in comparison with 1.466 in $\mathbf{TS_{C\text{-}C6}}$), in line with the strongest exothermicity of the reaction and the Hammond postulate. This structural feature is in fact associated with absence of activation of the $C\gamma{=}C\delta$ bond in $\mathbf{I_J}$ (1.345 Å, which is similar to the free electrophile) as expected in absence of interaction between the metal center and the double bond. We can thus propose that this mechanism, in which $\mathbf{I_J}$ is a non transmetalated species, is not effective because i) copper cannot act as an efficient Lewis acid and ii) there is no activation of the C=C bond in $\mathbf{I_J}$.

Accepted Manuscript

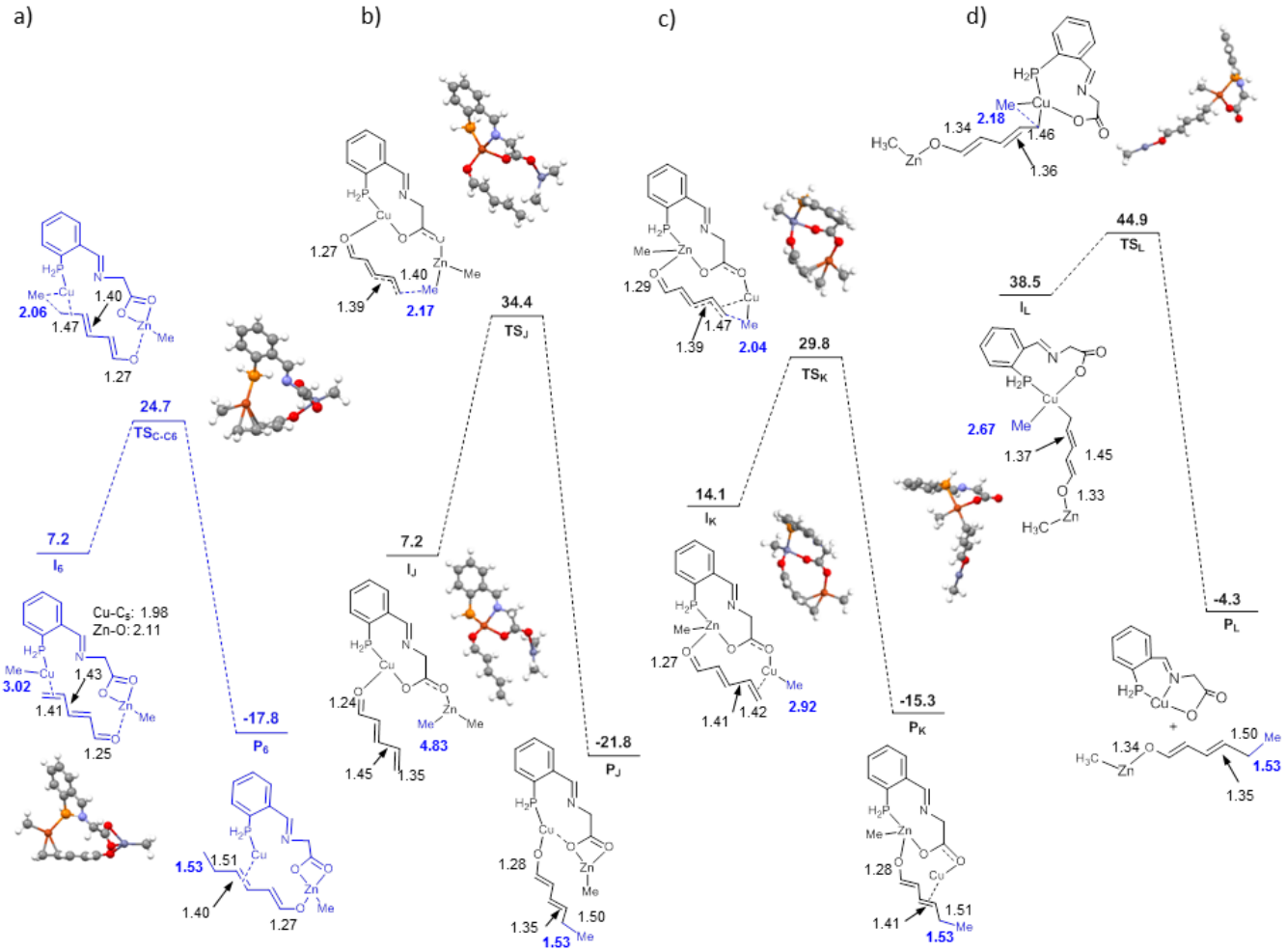

Figure 7. Gibbs free energy profile (in kcal mol^{-1}) for the three alternative mechanisms envisioned: proposed intermediate (a), non transmetalated species noted **I$_J$** (b), lateral Cu noted **I$_K$** (c) and separated ion pair noted **I$_L$** (d) (ΔG are computed with respect to separated reactants **1c,** $ZnMe_2$ and **Cu(M)**).

Mechanism through K. As the docking of the carbonyl compound takes place in a transmetalated species (only one alkyl group on Zn), the roles of the two metal centers in **I$_K$** are very similar to those in **I$_6$**: Cu is a C=C bond activator and Me donor while Zn, coordinated to the carbonyl compound, acts as a Lewis acid. The docking of the substrate in **I$_K$** is also similar to that stated in **I$_6$,** with the coordination of C=O to Zn and C=C bond to Cu. Nevertheless, due to the exchange of the bonding environment in **I$_6$** and **I$_K$**, the Cγ=Cδ bond distance (1.421 Å) is longer in **K** than that obtained in **I$_6$** (1.410 Å) suggesting that the coordination of Cu to the carboxylate arm of **M** increases its activating potential, in line with an anionic cuprate formal charge and thus a cuprate character in this intermediate. Consistently, the C-C bond formation exhibits a lower activation barrier with respect to the docking intermediate (15.7 kcal.mol^{-1} in Figure 7, c compared to 17.5 kcal.mol^{-1} calculated above). Increasing the cuprate character and Lewis acidity favor kinetically the step of C-C bond forming (**TS$_K$**). Nevertheless, the metal bonding environments are less favorable because **I$_K$** is found to be 5.9 kcal.mol^{-1} above **I$_6$**. It can be associated to the lowest stability of the bimetallic complex, as **C$_K$** is found to be significantly higher than **C$_0$** (+5.8 kcal.mol^{-1}). As a consequence, the decrease of the activation barrier between **I$_K$** and **TS$_K$** is lost by the destabilization of the adduct **I$_K$,** already evidenced in the bimetallic catalyst **C$_K$.**

Mechanism through L. The activation at stake in reaction path **K** relies on the synergetic double activation of the carbonyl compound by a Lewis acidic cation and a strong back donation of the electron rich copper center toward the C=C double bond.[26] To obtain the best of this effect, an "extreme" mechanism was thus searched using a ZnR^+ entity as an activating cation and docking the C=C double bond to the [Cu(**M**)R]$^-$ cuprate. The resulting docking intermediate is noted **I$_L$** in Figure 7, d. Intermediate **I$_L$** has a tetracoordinated geometry, in which the copper center is bonded to the phosphine and carboxylate groups of the ligand (**M**), to a methyl, and to the C$_δ$ terminal atom of substrate according to a short Cu-C$_δ$ distance of 2.017 Å. The square planar geometry of Cu and the pyramidalization of C$_δ$ in **I$_L$** confirms a strong back-donation of copper toward the dienone and thus a Cu(III) nature of the intermediate. The efficiency of this electron transfer in activating the electrophile is confirmed by the small activation barrier for C-

Accepted Manuscript

C bond formation (6.4 kcal.mol^{-1}), which is found to be 9.3 kcal.mol^{-1} lower than the smallest found up to now, in the case of mechanism **K**.

Nevertheless, intermediate $\mathbf{I_L}$ is very high in energy relative to $\mathbf{I_6}$ (+31.3 kcal.mol^{-1})**,** as could be expected from the decoordination of the Zn center from the DiPPAM ligand**.** Considering that this is associated to a very strong Lewis acidity of the $ZnMe^+$ entity and that the reaction takes place experimentally in ethereal solvent, an explicitly solvated model must be used to counterbalance this decoordination. Two molecules of dimethylether, as a model of solvent, namely MeTHF, are added to the $ZnMe^+$ moiety and decrease the energies of $\mathbf{I_L}$, $\mathbf{TS_L}$ and $\mathbf{P_L}$ by 10 kcal.mol^{-1} with respect to their analogues in gas phase (See SI, Table S7). Addition of single point implicit solvation to the latest model does not change the conclusions and mechanism through **L** remains higher than in our proposed mechanism (See SI, Table S7).

As a conclusion, we have examined four bimetallic mechanisms, using either Zn (mechanism **J**) or Cu as a nucleophilic center. The absence of C=C activation in the former increases significantly its activation barrier and disfavors this pathway. The three nucleophilic-Cu mechanisms differ by an increasing cuprate character, which is associated with lowering of activation barrier. Nevertheless, associated intermediates are at the same time destabilized. It thus appears that the preferred reaction pathway results from an equilibrium between the stability of the adduct and the activation of the substrate.

Conclusions

In this paper, the Cu-Zn bimetallic pathway and the resulting selectivity (regio- and enantioselectivity) of the Cu-catalyzed conjugate addition reaction of dialkylzinc to acyclic dienones are investigated by DFT calculations. The 1,6-addition is the kinetically and thermodynamically favored step, unless the conjugation of the α-β-γ-δ-dienone chain is altered by a terminal phenyl group. Furthermore, the retained bimetallic model allows the theoretical prediction of the absolute configuration, which was confirmed experimentally by converting a 1,6-adduct formed in the Cu/L-DiPPAM catalyzed ACA into a known chiral product. As this bimetallic mechanism seems general and proved compatible with different ligands (DiPPAM and NHC ligands) and various substrate types (cyclic and acyclic with different substituents), different competing pathways are considered to understand the factors that govern the mechanism. This confirms not only that the copper has to be a C=C bond activator and an alkyl donor while zinc plays the role of a Lewis acid which stabilizes the enolate during the C-C bond formation step but also that the C=C bond activation lowers that activation barrier of the C-C bond formation step. However, developing a strong Lewis acidity toward Zn and electronically enriching Cu appears energetically costly. As a consequence, the catalytic pathway appears as a balance between the stable neutral bimetallic complex and the activating ion-pair formation.

Experimental Section

Experimental Details. Compound **4** was prepared according to a slightly modified described procedure.[37] Compound **2a** (164.5 mg, 0.815 mmol, 85% ee) was dissolved along with K_2CO_3 (56 mg, 0.407 mmol) in a mixture of t-BuOH (40 mL) and distilled water (9 mL). A solution of K_2CO_3 (56 mg, 0.407 mmol), $NaIO_4$ (732.1 mg, 3.423 mmol) and $KMnO_4$ (32.2 mg, 0.204 mmol) in distilled water (31 mL) was added and the mixture was stirred at rt for 16 h. The reaction media was acidified to pH = 2 by adding HCl (1N) and then stirred another 6 h. Afterwards, $Na_2S_2O_5$ was added until disappearance of the reddish color. The mixture was extracted with Et_2O (100 mL) and the aqueous layer was removed. The organic layer was extracted with a 1M K_2CO_3 aqueous solution (100 mL) and after separation, the pH of the aqueous layer was lowered to 1 by a carefully addition of concentrated HCl (strong gas release). Finally, the aqueous layer was extracted with Et_2O (3x100 mL) and the combined organic layers were dried over $MgSO_4$, filtered and concentrated under reduced pressure (20°C, 520 mbar). The crude mixture, containing both carboxylic acids formed in this step, was directly used in the next step. The phenyldiazomethane in toluene solution was obtained according to Biffis' procedure.[40] To the mixture of the two carboxylic acids previously obtained was added 13 mL (2 equiv) of the phenyldiazomethane solution and the red mixture was stirred at rt for 16 h (persistence of the reddish color after this time). The mixture was concentrated under reduced pressure and purified by silica gel chromatography using a deposit solid (pentane/EtOAc: 100/0 to 80/20 Snap ultra 10g, Biotage puriflash). Many purifications were performed in order to obtain a fraction of **4** having an acceptable purity (25 mg; 16% yield over 2 steps, slightly yellow oil). $[\alpha]_D^{21}$ = +6.0 (c 1.0, $CHCl_3$).

Computational Details. The calculations were carried out with the Gaussian09 package.[41] All geometries and frequencies were obtained using the Density Functional Theory (DFT) with the hybrid B3PW91 functional.[42,43] This method is believed to be appropriate despite the bimetallic character of the studied complexes since both Cu(I) and Zn(II) centers are d^{10} closed-shell and are never in direct interaction. The copper, zinc metals and phosphorous were represented with the quasi-relativistic SDD ECP[44,45] completed by the associated basis-set.[46,47] A 6-31G(d,p) basis set was used for all other atoms (H, C, N, O, P).[48,49] Geometry optimizations were performed without any constraint and the nature of the extrema (minima and transition state) were verified by analytical calculations of frequencies. In addition, the connections between the transition state and minima were verified by carrying out a small displacement along the reaction coordinate in each direction and optimizing geometry starting from these structures. The Gibbs free energies were calculated assuming an ideal gas, unscaled harmonic frequencies, and the rigid rotor approximation in the standard conditions (P = 1 atm and T = 298 K). Dispersion effects were examined for the complete system with the hybrid B3PW91-D3 corrected functional.[50] A single point evaluation was carried out on all the stationary points of the 1,4 and 1,6 reaction pathways (see S.I. Table S8) and confirmed that dispersion effects don't alter our conclusions. For the enantioselectivity aspects, geometry optimizations were directly carried out including dispersion. To illustrate weak interactions, Non Covalent interactions isosurfaces were obtained with NCIPLOT code.[51,52] For alternative mechanisms part, copper and zinc metals were represented with the quasi-relativistic SDD ECP[44] completed by the associated basis-set.[46] A 6-31++G(d,p) basis set was used for all other atoms (H, C, N, O, P).[48,49] In addition, Density-based Solvation Model (SMD)[53] was used as it is considered as a good method to calculate the free energy of solvation ΔG_{solv} for neutral and ionic molecules in solvent (mean unsigned errors of 1 kcal.mol^{-1} for neutral molecules). SMD Single point calculations (THF is used) are given in the solvent molecule (Me_2O instead of MeTHF) as a supermolecule, was used as the second method of solvation model.

Acknowledgements

This work was supported by the Agence Nationale de la Recherche (SCATE grant no. ANR 12-BS07-0009-01). The authors thank Pr. A. Alexakis for fruitul discussions.

Accepted Manuscript

Keywords: C-C bond • DFT • catalysis • Cu/Zn heterobimetallic active species • enantioselectivity

[1] A. Alexakis, N. Krause, S. Woodward, Eds. , *Copper-Catalyzed Asymmetric Synthesis*, Wiley-VCH Verlag GmbH & Co. KGaA, Weinheim, Germany, **2014**.

[2] A. D.-N. M. Mauduit O. Baslé, H. Clavier, C. Crévisy, in *Compr. Org. Synth.* (Ed.: P.K. G. A. Molander), Elsevier: Oxford, **2014**, pp. 189–341.

[3] H. Hénon, M. Mauduit, A. Alexakis, *Angew. Chemie Int. Ed.* **2008**, *47*, 9122–9124.

[4] K. Lee, A. H. Hoveyda, *J. Am. Chem. Soc.* **2010**, *132*, 2898–2900.

[5] J. Wencel-Delord, A. Alexakis, C. Crévisy, M. Mauduit, *Org. Lett.* **2010**, *12*, 4335–4337.

[6] T. Nishimura, Y. Yasuhara, T. Sawano, T. Hayashi, *J. Am. Chem. Soc.* **2010**, *132*, 7872–7873.

[7] M. Magrez, J. Wencel-Delord, A. Alexakis, C. Crévisy, M. Mauduit, *Org. Lett.* **2012**, *14*, 3576–3579.

[8] T. Nishimura, A. Noishiki, T. Hayashi, *Chem. Commun.* **2012**, *48*, 973–975.

[9] M. Tissot, D. Poggiali, H. Hénon, D. Müller, L. Guénée, M. Mauduit, A. Alexakis, *Chem. - A Eur. J.* **2012**, *18*, 8731–8747.

[10] J. Wencel, D. Rix, T. Jennequin, S. Labat, C. Crévisy, M. Mauduit, *Tetrahedron Asymmetry* **2008**, *19*, 1804–1809.

[11] M. Magrez-Chiquet, M. S. T. Morin, J. Wencel-Delord, S. Drissi Amraoui, O. Baslé, A. Alexakis, C. Crévisy, M. Mauduit, *Chem. - A Eur. J.* **2013**, *19*, 13663–13667.

[12] T. E. Schmid, S. Drissi-Amraoui, C. Crévisy, O. Baslé, M. Mauduit, *Beilstein J. Org. Chem.* **2015**, *11*, 2418–2434.

[13] M. Morin, T. Vives, O. Baslé, C. Crévisy, V. Ratovelomanana-Vidal, M. Mauduit, *Synthesis* **2015**, *47*, 2570–2577.

[14] S. R. Krauss, S. G. Smith, *J. Am. Chem. Soc.* **1981**, *103*, 141–148.

[15] C. Ullenius, B. L. Christenson, *Pure Appl. Chem.* **1988**, *60*, 57–64.

[16] A. S. Vellekoop, R. A. J. Smith, *J. Am. Chem. Soc.* **1994**, *116*, 2902–2913.

[17] N. Krause, R. Wagner, A. Gerold, *J. Am. Chem. Soc.* **1994**, *116*, 381–382.

[18] R. M. Gschwind, *Chem. Rev.* **2008**, *108*, 3029–3053.

[19] N. Krause, A. Gerold, *Angew. Chem. Int. Ed Eng.* **1997**, *36*, 186–204.

[20] J. Canisius, A. Gerold, N. Krause, *Angew. Chem. Int. Ed* **1999**, *38*.

[21] E. Nakamura, S. Mori, K. Morokuma, *J. Am. Chem. Soc.* **1997**, *119*, 4900–4910.

[22] S. Mori, E. Nakamura, *Chem. - A Eur. J.* **1999**, *5*, 1534–1543.

[23] E. Nakamura, S. Mori, *Angew. Chem. Int. Ed.* **2000**, *39*, 3750–3771.

[24] S. Woodward, *Chem. Soc. Rev.* **2000**, *29*, 393–401.

[25] S. Mori, E. Nakamura, in *Mod. Organocopper Chem.*, Wiley-VCH Verlag GmbH, Weinheim, FRG, **n.d.**, pp. 315–346.

[26] N. Yoshikai, E. Nakamura, *Chem. Rev.* **2012**, *112*, 2339–2372.

[27] M. Yan, L. W. Yang, K. Y. Wong, A. S. C. Chan, *Chem. Commun.* **1999**, 11–12.

[28] B. L. F. S. R. Harutyunyan, F. López, W. R. Browne, A. Correa, D Peña, R. Badorrey, A. Meetsma, A. J. Minnaard, *J. Am. Chem. Soc.* **2006**, *128*, 9103–9118.

[29] F. von Rekowski, C. Koch, R. M. Gschwind, *J. Am. Chem. Soc.* **2014**, *136*, 11389–11395.

[30] M. Welker, S. Woodward, L. F. Veiros, M. J. Calhorda, *Chem. - A Eur. J.* **2010**, *16*, 5620–5629.

[31] S. Drissi-Amraoui, T. E. Schmid, J. Lauberteaux, C. Crévisy, O. Baslé, R. M. de Figueiredo, S. Halbert, H. Gérard, M. Mauduit, J.-M. Campagne, *Adv. Synth. Catal.* **2016**, *358*, 2519–2540.

[32] C. Blons, M. S. T. Morin, T. E. Schmid, T. Vives, S. Colombel-Rouen, O. Baslé, T. Reynaldo, C. L. Covington, S. Halbert, S. N. Cuskelly, P. V. Bernhardt, C. M. Williams, J. Crassous, P. L. Polavarapu, C. Crévisy, H. Gérard, M. Mauduit, *Chem. - A Eur. J.* **2017**, *23*, 7515–7525.

[33] A. Hajra, N. Yoshikai, E. Nakamura, *Org. Lett.* **2006**, *8*, 4153–4155.

[34] E. N. Yoshikai, T. Yamashita, Nakamura, *Chem. – Asian J.* **2006**, *1*, 322–330.

Accepted Manuscript

[35] A. Alexakis, J. E. Bäckvall, N. Krause, O. Pàmies, M. Diéguez, *Chem. Rev.* **2008**, *108*, 2796–2823.

[36] T. den Hartog, B. Maciá, A. J. Minnaard, B. L. Feringa, *Adv. Synth. Catal.* **2010**, *352*, 999–1013.

[37] X. Huo, M. Quan, G. Yang, X. Zhao, D. Liu, Y. Liu, W. Zhang, *Org. Lett.* **2014**, *16*, 1570–1573.

[38] A. Wooten, P. J. Carroll, A. G. Maestri, P. J. Walsh, *J. Am. Chem. Soc.* **2006**, *128*, 4624–4631.

[39] S. Halbert, H. Gérard, *New J. Chem.* **2015**, *39*, 5410–5419.

[40] M. Verdecchia, C. Tubaro, A. Biffis, *Tetrahedron Lett.* **2011**, *52*, 1136–1139.

[41] Gaussian 09, Revision D.01, M. J. Frisch, G. W. Trucks, H. B. Schlegel, G. E. Scuseria, M. A. Robb, J. R. Cheeseman, G. Scalmani, V. Barone, G. A. Petersson, H. Nakatsuji, X. Li, M. Caricato, A. Marenich, J. Bloino, B. G. Janesko, R. Gomperts, B. Mennucci, H. P. Hratchian, J. V. Ortiz, A. F. Izmaylov, J. L. Sonnenberg, D. Williams-Young, F. Ding, F. Lipparini, F. Egidi, J. Goings, B. Peng, A. Petrone, T. Henderson, D. Ranasinghe, V. G. Zakrzewski, J. Gao, N. Rega, G. Zheng, W. Liang, M. Hada, M. Ehara, K. Toyota, R. Fukuda, J. Hasegawa, M. Ishida, T. Nakajima, Y. Honda, O. Kitao, H. Nakai, T. Vreven, K. Throssell, J. A. Montgomery, Jr., J. E. Peralta, F. Ogliaro, M. Bearpark, J. J. Heyd, E. Brothers, K. N. Kudin, V. N. Staroverov, T. Keith, R. Kobayashi, J. Normand, K. Raghavachari, A. Rendell, J. C. Burant, S. S. Iyengar, J. Tomasi, M. Cossi, J. M. Millam, M. Klene, C. Adamo, R. Cammi, J. W. Ochterski, R. L. Martin, K. Morokuma, O. Farkas, J. B. Foresman, and D. J. Fox, Gaussian, Inc., Wallingford CT, **2016**.

[42] J. P. Perdew, Y. Wang, *Phys. Rev. B* **1992**, *45*, 13244–13249.

[43] A. D. Becke, *J. Chem. Phys.* **1993**, *98*, 5648–5652.

[44] D. Andrae, U. Häussermann, M. Dolg, H. Stoll, H. Preuss, *Theor. Chim. Acta* **1990**, *77*, 123–141.

[45] A. Bergner, M. Dolg, W. Küchle, H. Stoll, H. Preuß, *Mol. Phys.* **1993**, *80*, 1431–1441.

[46] A. W. Ehlers, M. Böhme, S. Dapprich, A. Gobbi, A. Höllwarth, V. Jonas, K. F. Köhler, R. Stegmann, A. Veldkamp, G. Frenking, *Chem. Phys. Lett.* **1993**, *208*, 111–114.

[47] A. Höllwarth, M. Böhme, S. Dapprich, A. W. Ehlers, A. Gobbi, V. Jonas, K. F. Köhler, R. Stegmann, A. Veldkamp, G. Frenking, *Chem. Phys. Lett.* **1993**, *208*, 237–240.

[48] W. J. Hehre, R. Ditchfield, J. A. Pople, *J. Chem. Phys.* **1972**, *56*, 2257–2261.

[49] M. M. Francl, W. J. Pietro, W. J. Hehre, J. S. Binkley, M. S. Gordon, D. J. DeFrees, J. A. Pople, *J. Chem. Phys.* **1982**, *77*, 3654–3665.

[50] S. Grimme, J. Antony, S. Ehrlich, H. Krieg, *J. Chem. Phys.* **2010**, *132*, 154104.

[51] E. R. Johnson, S. Keinan, P. Mori-Sánchez, J. Contreras-García, A. J. Cohen, W. Yang, *J. Am. Chem. Soc.* **2010**, *132*, 6498–6506.

[52] J. Contreras-García, E. R. Johnson, S. Keinan, R. Chaudret, J. P. Piquemal, D. N. Beratan, W. Yang, *J. Chem. Theory Comput.* **2011**, *7*, 625–632.

[53] A. V. Marenich, C. J. Cramer, D. G. Truhlar, *J. Phys. Chem. B* **2009**, *113*, 6378–6396.

Accepted Manuscript

FULL PAPER

Copper/DiPPAM-catalyzed 1,6-Asymmetric Conjugate Addition (ACA) of dialkylzinc to acyclic dienones pathway is demonstrated to originate from a balance between the activating potential of the two Cu and Zn centers and the stability of the bimetallic complex. The retained mechanism is supported by the experimentally observed regio- and enantioselectivities.

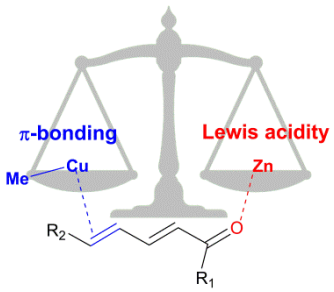

Stéphanie Halbert, Jimmy Lauberteaux, Charlie Blons, Renata Marcia de Figueiredo, Christophe Crévisy, Olivier Baslé, Jean-Marc Campagne, Marc Mauduit and Hélène Gérard

Page No. – Page No.

Catalytically active species in Copper/DiPPAM-Catalyzed 1,6-Asymmetric Conjugate Addition of Dialkylzinc to Dienones: a computational overview.

Accepted Manuscript